Journal of Power Sources 191 (2009) 377–383

Contents lists available at ScienceDirect

Journal of Power Sources

journal homepage: www.elsevier.com/locate/jpowsour

Improved electrical performance and sintering ability of the composite interconnect $La_{0.7}Ca_{0.3}CrO_{3-\delta}/Ce_{0.8}Nd_{0.2}O_{1.9}$ for solid oxide fuel cells

Xiaoliang Zhou[a,b,c,*], Peng Wang[b,**], Limin Liu[c], Kening Sun[a,c], Zhiqiang Gao[d], Naiqing Zhang[a,c]

[a] Science Research Center, Academy of Fundamental and Interdisciplinary Sciences, Harbin Institute of Technology, Harbin 150080, PR China
[b] School of Municipal and Environmental Engineering, Harbin Institute of Technology, Harbin 150090, PR China
[c] Department of Applied Chemistry, Harbin Institute of Technology, No. 92 of West Dazhi Street, P.O. Box 211, Harbin 150001, PR China
[d] Department of Microelectronics, Harbin Institute of Technology, Harbin 150001, PR China

ARTICLE INFO

Article history:
Received 17 January 2009
Received in revised form 22 February 2009
Accepted 23 February 2009
Available online 6 March 2009

Keywords:
Doped ceria
Electrical property
Auto-ignition process
Interconnect
SOFC

ABSTRACT

Significant improvements on sintering characteristic and electrical performance of traditional interconnect $La_{0.7}Ca_{0.3}CrO_{3-\delta}$ were presented in this paper. For a composite interconnecting ceramic $La_{0.7}Ca_{0.3}CrO_{3-\delta}/Ce_{0.8}Nd_{0.2}O_{1.9}$, it was found that the addition of $Ce_{0.8}Nd_{0.2}O_{1.9}$ significantly increased the electrical conductivity of $La_{0.7}Ca_{0.3}CrO_{3-\delta}$ both in air and in hydrogen. Among all the investigated specimens, $La_{0.7}Ca_{0.3}CrO_{3-\delta}$ with 5 wt% $Ce_{0.8}Nd_{0.2}O_{1.9}$ possessed the maximal electrical conductivity. In air and hydrogen, the maximal electrical conductivity at 800 °C were 55.4 S cm^{-1} and 5.0 S cm^{-1}, respectively, which increased significantly as compared with $La_{0.7}Ca_{0.3}CrO_{3-\delta}$ under the same conditions. With the increase of $Ce_{0.8}Nd_{0.2}O_{1.9}$ content the relative density increased, reaching 97.1% from 93.9% of $La_{0.7}Ca_{0.3}CrO_{3-\delta}$. This indicated that $Ce_{0.8}Nd_{0.2}O_{1.9}$ functioned as an effective sintering aid in enhancing the sinterability of the powders. The average coefficient of thermal expansion at 30–1000 °C in air increased with $Ce_{0.8}Nd_{0.2}O_{1.9}$ content. Most coefficients of thermal expansion of specimens are compatible with other cell components. The oxygen permeation measurement illustrated a negligible oxygen ionic conduction, indicating it is still an electronically conducting ceramic. Results indicate that this composite is suitable to be used as a high-performance interconnect for intermediate temperature solid oxide fuel cells.

1. Introduction

Solid oxide fuel cells (SOFCs) are promising candidates for many power generation schemes from small systems of a few watts up to megawatt-sized power plants and have been considered as the premium power generation devices in the future. They have demonstrated high energy conversion efficiency, high power density, extremely low pollution, in addition to flexibility in using hydrocarbon fuel [1]. One of the recent significant advancements in SOFC development is the reduction of its operating temperature from about 1000 °C to the range of 600–800 °C [2–7]. To accumulate the voltage output, multiple cells are electrically connected into series via interconnects. A major materials challenge in SOFC development is the interconnect material, which provides the conductive path for electrical current to pass between the electrodes and to the external circuit [8–10]. The interconnect material clearly must have good electrical conductivity to minimize ohmic losses. The interconnect material operates at high temperatures, therefore it should have a coefficient of thermal expansion (CET), which is close to those of the other cell components to minimize thermal stresses. Other requirements for interconnect materials include adequate mechanical strength, low permeability to oxygen and hydrogen, and reasonable thermal conductivity. In addition, cost-effective manufacture of fuel cells requires that the interconnect materials be easy to fabricate. These rigorous requirements eliminate all but only a few oxide systems from consideration for SOFC interconnect. High-temperature alloys have also been considered as interconnect materials, but can only be used for flat-plate SOFCs operated below 850 °C.

$LaCrO_3$-based perovskite materials have been widely investigated as the ceramic interconnects for SOFCs owing to their thermal and chemical stability and high electrical conductivity at both reducing and oxidizing atmospheres [11–14]. However, due to the strong dependence of electrical conductivity on the oxygen pressure, the electrical conductivity of the doped $LaCrO_3$ in the reducing atmosphere like hydrogen is significantly lower than that in the oxidizing atmosphere like air [15]. As such, a conductivity gradient

* Corresponding author at: School of Municipal and Environmental Engineering, Harbin Institute of Technology, Harbin 150090, PR China. Tel.: +86 451 86412153; fax: +86 451 86412153.
** Corresponding author. Tel.: +86 451 86412153; fax: +86 451 86412153.
E-mail addresses: xlzhou.hit@gmail.com (X. Zhou), pwang@hit.edu.cn (P. Wang).

0378-7753/$ – see front matter © 2009 Elsevier B.V. All rights reserved.
doi:10.1016/j.jpowsour.2009.02.071

across the doped $LaCrO_3$ is established when it is utilized as an interconnect in a SOFC, considering that it is subjected to fuel on one side and oxidant on the other. Fortunately, the overall conductivity of the doped $LaCrO_3$ is still sufficient for its use as long as the operating temperature is above 800 °C [9]. However, at temperatures below 800 °C, the electrical conductivity of doped $LaCrO_3$ is reported to experience substantial degradation [16]. This limitation renders it virtually useless for intermediate temperatures 600–800 °C.

To improve the sinterability of doped $LaCrO_3$, several methods have been adopted. (1) Sintering in reducing atmosphere, followed by oxidation treatment to restore its high electrical conductivity. This can effectively densify the material at a relatively lower temperature. However, this method is high-cost and rather difficult to control. (2) Addition of sintering aids. Liquid-phase sintering aids can effectively encourage densification of $LaCrO_3$ in oxidizing environments. Sintering aids such as Bi_2O_3 and some fluorides like LaF_3, YF_3, and MgF_2 have been used to densify $LaCrO_3$ at relatively lower temperatures [17,18]. However, the main difficulty involving sintering aids is that they may migrate to other cell components, causing elemental migration and morphological changes. (3) By using uniform and highly reactive powders. A newly developed synthesis method called auto-ignition process can effectively enhance the density and phase purity of the ceramic materials at lower temperature [14,19,20].

The work reported in this communication aims at developing novel interconnect materials with higher sintering ability and higher electrical conductivities in both air and pure hydrogen at relatively low temperatures. This is a critical step toward making SOFCs affordable for a wide variety of applications. In this communication, we report our recent advance in preparation and properties of LCC ($La_{0.7}Ca_{0.3}CrO_{3-\delta}$) with an addition of the electrolyte NDC ($Ce_{0.8}Nd_{0.2}O_{1.9}$) in an effort to significantly reduce the operating temperature. Sintering behavior, electrical conductivities and thermal expansion of LCC + NDC were investigated.

2. Experimental details

2.1. The preparation of powders NDC and LCC

In order to prepare 20 mol% Nd_2O_3-doped CeO_2 powders by GNP (glycine nitrate process), stoichiometric amounts of $Ce(NO_3)_3{\cdot}6H_2O$ (99.9% AR) and neodymium oxide (Nd_2O_3) (99.99% AR) were dissolved in nitric acid (all analytical reagents, Sinopharm Chemical Reagent Co., Ltd.). Glycine was added as the complexing agent to the above solution. The amount of glycine added was such that the ratio of total number of moles of cations to that of glycine was 1:1.2. After spontaneous ignition, the resultant red-brown ash was collected and calcined in air at 800 °C for 2 h to remove any carbon residue remained in the oxide powder.

The $La_{0.7}Ca_{0.3}CrO_{3-\delta}$ powders were synthesized by auto-ignition process. The starting materials, calcium nitrate ($Ca(NO_3)_2{\cdot}4H_2O$) (99.9% AR), lanthanum oxide (La_2O_3) (99.99% AR) and chromic nitrate ($Cr(NO_3)_3{\cdot}6H_2O$) (99.9% AR), were mixed with three times as much citric acid in distilled water. The mixture was then heated to form a gel and the wet gel was further heated to about 120 °C to remove the solvents. The dried gel was placed in an oven at 650 °C. The combustion reaction took place within a few seconds, forming the primary powder. The as-synthesized powders were calcined at 650 °C for 2 h.

2.2. The preparation of specimens LCC + NDC

The fine powders with the composition of LCC + x wt%NDC (x = 0, 1, 3, 5, 7 and 9) were ball-milled in ethanol medium overnight and dried subsequently. Small pellets and rectangular bar specimens were then produced by pressing at 360 MPa and sintered in air at 1400 °C for 4 h. The heating rate was fixed at 1 °C min^{-1} before 550 °C and 2 °C min^{-1} between 550 °C and 1400 °C.

2.3. Analysis and characterization

Various phases of the sintered specimens were identified by X-ray diffraction analysis on a Philips PW 1730 diffractometer using Cu Kα radiation. Particle size and fractured surfaces of the sintered specimens were observed by scanning electron microscopy (Hitachi X-650 and XT30 ESEM-TMP). The electrical conductivity of the materials was studied from 450 °C to 850 °C using a standard DC four-probe technique on a H.P. multimeter (Model 34401). The bulk density of all the sintered specimens was measured by liquid displacement method using toluene. The thermal expansion was measured at 30–1000 °C on cylindrical rods of the sintered specimens using a dilatometer (SHIMADZU50) at a heating rate of 5 °C min^{-1}. The oxygen penetration flux was measured by gas chromatography.

3. Results and discussion

3.1. XRD phase structure analysis

X-ray diffraction patterns of NDC powders calcined at 650 °C for 2 h and LCC powders with different NDC content x wt% (x = 0, 3, 5, 7 and 9) calcined at 1400 °C for 4 h are shown in Fig. 1. The XRD patterns of the NDC specimen displayed all peaks associated with those of a pure fluorite structure. The LCC specimen showed a pure perovskite phase with an orthorhombic symmetry. In other specimens, the NDC content ranged from 3 wt% to 9 wt% and the phase structures of LCC and NDC did not change after sintering at 1400 °C for 4 h. At lower NDC content, there was no evident NDC phase in the XRD. This may result from the fact that the NDC dissolved into LCC structure and formed one phase with LCC. However, it is also possible that NDC still existed in the form of a pure fluorite structure since XRD commonly has a detection limit of ~5%.

3.2. SEM analysis and relative density measurements

The SEM images of the specimens in Fig. 2 showed that dense materials were fabricated in air after sintering, indicating that the as-prepared powders were sinterable. As shown in Fig. 2, clear grain

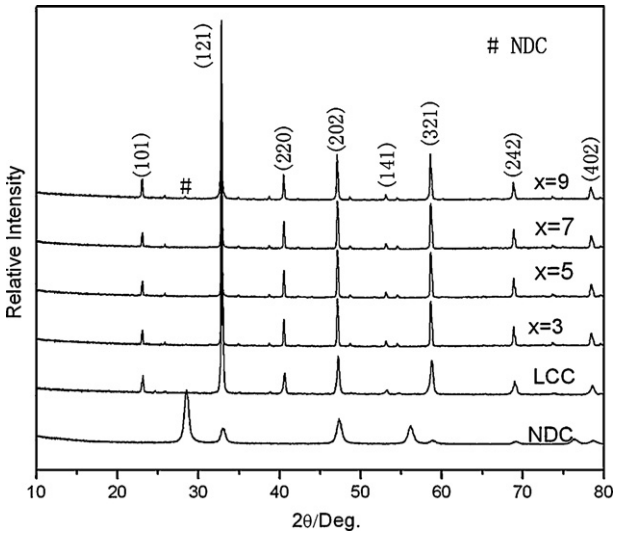

Fig. 1. X-ray diffraction patterns of NDC powders calcined at 650 °C for 2 h and LCC powders with different NDC content x wt% (x = 0, 3, 5, 7 and 9) calcined at 1400 °C for 4 h.

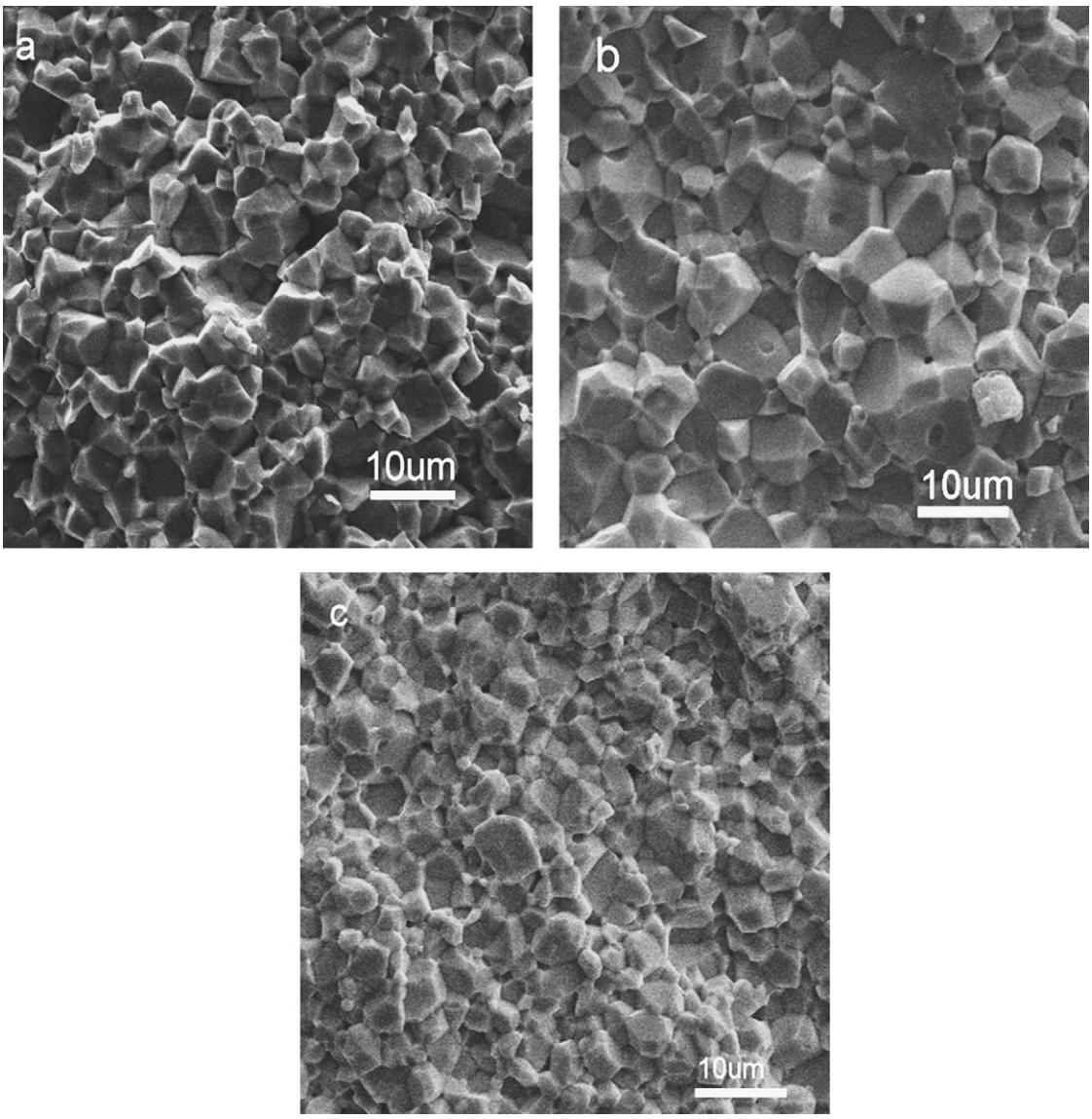

Fig. 2. The SEM images of the specimens sintered at 1400 °C for 4 h: panels a, b and c show LCC, LCC + 5 wt%NDC and LCC + 9 wt%NDC, respectively.

boundaries were observed. This feature of the microstructure usually appears in the dense sintered body. The average grain sizes of the different specimens ranged from 2 μm to 8 μm. Fig. 2(a) shows that the average grain size was 4 μm when the specimen contained no NDC. When the NDC content was 5 wt%, the average grain sizes possessed the maximal average size of 8 μm as shown in Fig. 2(b). Instead of increasing as when the NDC content was ranged from 0 wt% to 5 wt%, the average grain size deceased once the NDC content further increased. The average grain sizes for the specimen LCC + 9 wt%NDC were smaller than that of the specimen with 5 wt%NDC as shown in Fig. 2(c). Combining with the XRD phase structure analysis in Fig. 1, it can be concluded that the existence of NDC thus restrained the growth of grains. The influence of NDC content on relative density of different specimens is shown in Fig. 3 and Table 1. With the increase of NDC content from 0 wt% to 9 wt%, the relative density increased to a great extent. The relative density of the specimen LCC was 93.9% when sintered at 1400 °C for 4 h. The addition of NDC powder into LCC remarkably enhanced the relative density. When the NDC content was 5 wt%, the relative density was 96.5%. Further increasing the NDC content to 9 wt%, the relative den-

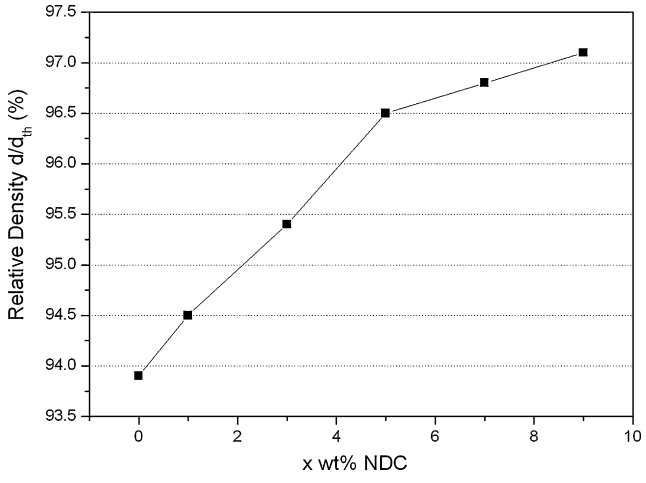

Fig. 3. The influence of NDC content on relative density of different specimens.

Table 1
Characteristics of the composite interconnect LCC + NDC.

NDC content (x wt%)	Electrical conductivity in air at 800 °C ($S\,cm^{-1}$)	Electrical conductivity in air at 500 °C ($S\,cm^{-1}$)	Electrical conductivity in hydrogen at 800 °C ($S\,cm^{-1}$)	Electrical conductivity in hydrogen at 500 °C ($S\,cm^{-1}$)	Activation energy in air (kJ mol^{-1})	Activation energy in hydrogen (kJ mol^{-1})	Relative density d/d_{th} (%)	Oxygen permeation flux (10^{-9} mol·s^{-1}·cm^{-2})
0	25.3	14.3	3.5	1.4	20.3	30.1	93.9	0.65
1	28.9	18.1	3.7	1.4	18.3	29.7	94.5	0.81
3	39.2	31.8	4.8	2.0	12.6	27.3	95.4	1.32
5	55.4	39.8	5.0	3.0	15.2	19.7	96.5	2.13
7	47.1	32.9	4.9	2.5	15.8	23.6	96.8	2.56
9	33.3	24.5	4.5	1.6	14.5	32.0	97.1	3.34

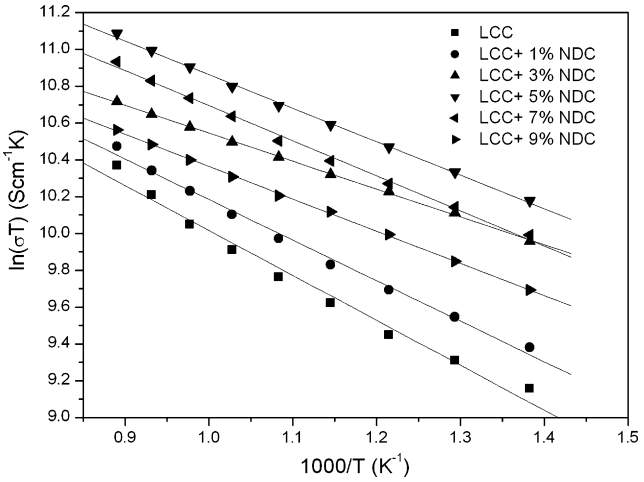

Fig. 4. Arrhenius plots of the electrical conductivities for the specimens with different NDC contents in air.

sity reached 97.1% after sintered at 1400 °C for 4 h. Therefore, NDC functioned as an effective sintering aid in accelerating the sintering ability of the powders.

3.3. Electrical conductivity

Arrhenius plots of the electrical conductivities for the specimens with different NDC contents in air are shown in Fig. 4. It can be seen that the electrical conductivities of the specimens with a specific NDC content increased with increasing temperature and reached a maximum at 850 °C. At each specific temperature studied, the electrical conductivities of the specimens reached a maximum when the specimen contained 5 wt% NDC as shown in Fig. 5 and Table 1. Therefore, the specimen with 5 wt% NDC possessed the maximum conductivity of 55.4 S cm^{-1} at 800 °C under these experimental conditions which is 2.2 times as high as that of the commonly used lanthanum chromite $La_{0.7}Ca_{0.3}CrO_{3-\delta}$ (25.3 S cm^{-1} at 800 °C). And it is note worthy that even at 500 °C, 600 °C and 700 °C, the electrical conductivities could reach 39.8 S cm^{-1}, 45.5 S cm^{-1} and 50.3 S cm^{-1}, respectively.

As shown in Fig. 4, all the LCC + NDC ceramics displayed linear conductivity behavior in the temperature range from 450 °C to 850 °C. The linear relationship between ln(σT) and 1/T indicates that the electrical conductivity behavior obeys the small polaron

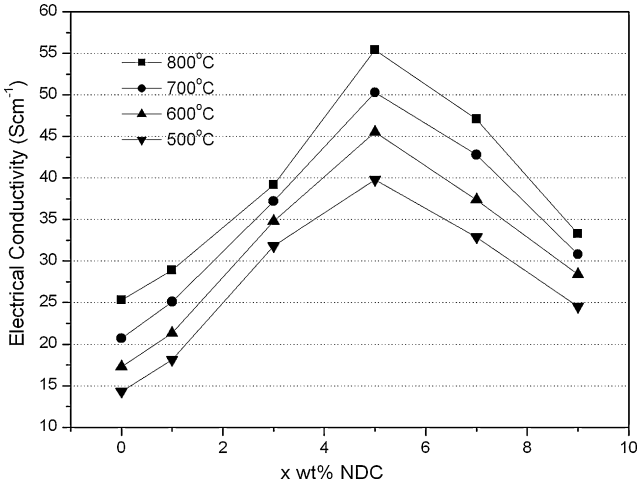

Fig. 5. Effect of NDC content on the electrical conductivity of the specimens in air at different temperatures.

conduction mechanism, as expressed in the following equation:

$$\sigma = \frac{A}{T}\exp\left(-\frac{Ea}{kT}\right) \quad (1)$$

where A is a pre-exponential factor, k the Boltzmann constant, T the absolute temperature, and Ea the activation energy for the conduction. The activation energies of all specimens in air are listed in Table 1. It can be seen that introduction of NDC into LCC decreased the activation energy for the conduction.

Earlier study [21] on $LaCrO_3$ indicates that it is a p-type conductor and electrical conduction occurs by the small polaron mechanism via transport of electron holes. A number of articles [21–27] have addressed the nature of the defect chemistry and electrical conductivity of Ca-doped $LaCrO_3$. Under high oxygen activity atmosphere, where oxygen pressure is typically larger than 10^{-8} atm, the negatively charged Ca'_{La} is electrically compensated by Cr^{3+} to Cr^{4+} transition in order to keep electroneutrality. The nature of the electrical conductivity of Ca-doped $LaCrO_3$, using the Kröger–Vink notion, can be described as the following equation:

$$[Ca'_{La}] = [Cr^{\bullet}_{Cr}] \quad (2)$$

where [] indicates concentration, $Cr_{Cr}^{\bullet}$ is Cr^{4+} in 3+ Cr-site. The electrical transport in doped $LaCrO_3$ is dominated by small-polaron hopping of charge carrier localized at the Cr sites. The ionic radii of Nd^{3+}, Ce^{4+}, La^{3+} and Cr^{3+} are 1.00 Å, 0.92 Å, 1.18 Å and 0.62 Å, respectively. As far as the ionic radii are concerned, Nd^{3+} and Ce^{4+} are prone to substitute the La^{3+} instead of the Cr^{3+}, finally resulting in the occurrence and increasing of Cr deficiency. Therefore, when a small amount of NDC was added into LCC, a portion of Nd and Ce ions substituted the La ion after sintering the specimens at 1400 °C for 4 h. However, as the increase of Cr deficiency, the concentration of Cr vacancy $[V'''_{Cr}]$ will increase. The negatively charged Cr vacancy might has the tendency to attract the positively charged $Cr_{Cr}^{\bullet}$ to keep micro-electroneutrality, so that the small-polaron hopping of $Cr_{Cr}^{\bullet}$ is confined, resulting in the electrical conductivity ability of the materials declining when the NDC content was more than 5 wt% as shown in Fig. 5 and Table 1. However, as the NDC content was less than 5 wt%, the electrical conductivity increased with the content. This may have resulted from an increase in density of the composite materials from 93.9% for $x = 0$ to 96.5% for $x = 5$.

At low oxygen activity conditions, such as in hydrogen, large amount of oxygen vacancy will be formed because of the escape of oxygen ion. The balance between the defect species and the surrounding atmosphere can be described through the following reaction:

$$O_O^{\times} + 2Cr_{Cr}^{\bullet} \leftrightarrow \frac{1}{2}O_2 + V_O^{\bullet\bullet} + 2Cr_{Cr}^{\times} \quad (3)$$

where $V_O^{\bullet\bullet}$ is oxygen vacancy and $Cr_{Cr}^{\times}$ represents Cr^{3+} in 3+ Cr site. In order to keep electroneutrality in the whole crystal, the following equation must be held:

$$[Ca'_{La}] = 2[V_O^{\cdot\cdot}] + [Cr'_{Cr}] \quad (4)$$

This means that under reducing conditions, the lattice oxygen transforms into a doubly charged oxygen vacancy consuming two electron holes simultaneously. That is the reason why the electrical conductivity ability of the material deceases so sharply from in air to pure hydrogen atmosphere. Because the Cr vacancy concentration in the material increases with the increase of the Cr deficiency, Eq. (4) should be modified as the following equation:

$$[Ca'_{La}] + 3[V'''_{Cr}] = 2[V_O^{\bullet\bullet}] + [Cr^{\bullet}_{Cr}] \quad (5)$$

From above equation, it can be seen that the concentration of $Cr_{Cr}^{\bullet}$ will increase with the concentration increase of Cr vacancy, consequently resulting in the increase of the electrical conductivity ability of the material in hydrogen. Fig. 6 demonstrates Arrhenius plots of the electrical conductivities for the specimens with different NDC contents in hydrogen atmosphere. The linear relationship between $\ln(\sigma T)$ and $1/T$ indicates that the electrical conductivity behavior also obeys the small polaron conduction mechanism. The activation energies for the different specimens are listed in Table 1. Aside from the specimen with 9 wt% NDC, the activation energies of the other specimens decreased to some extent compared with the specimen without NDC. Fig. 7 shows the effect of NDC content on the electrical conductivity of the specimens in hydrogen at different temperatures. As such in the air, the electrical conductivity gradually increased with increasing NDC content up to 5 wt% in hydrogen. Subsequently, a sudden change in electrical conductivity occurred when the NDC content further increased. Probably this could be explained as the influence of a small amount (<5%) of second phases (NDC) showed up as the NDC content value reached up to 5 wt%. With attention to particulars, at 800 °C, the specimen with 5 wt% NDC has a maximum electrical conductivity of 5.0 S cm^{-1} which is also higher than that of the LCC ceramics (3.5 S cm^{-1}) as shown in Table 1. At 500 °C, 600 °C and 700 °C in hydrogen, the maximal values of the electrical conductivities reached 3.0 S cm^{-1}, 3.9 S cm^{-1} and 4.6 S cm^{-1}, respectively. These values are evidently higher than those of LCC under the same operating conditions. Since a value of 1 S cm^{-1} is a well-accepted minimum electrical conductivity for usefulness of interconnects in SOFC community [28], and

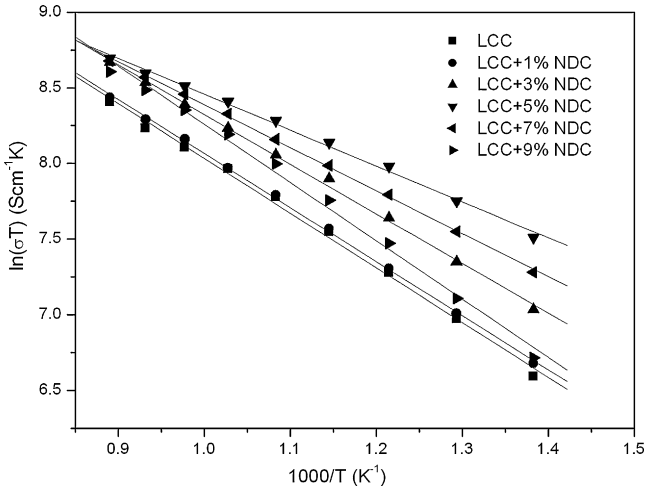

Fig. 6. Arrhenius plots of the electrical conductivities for the specimens with different NDC contents in hydrogen.

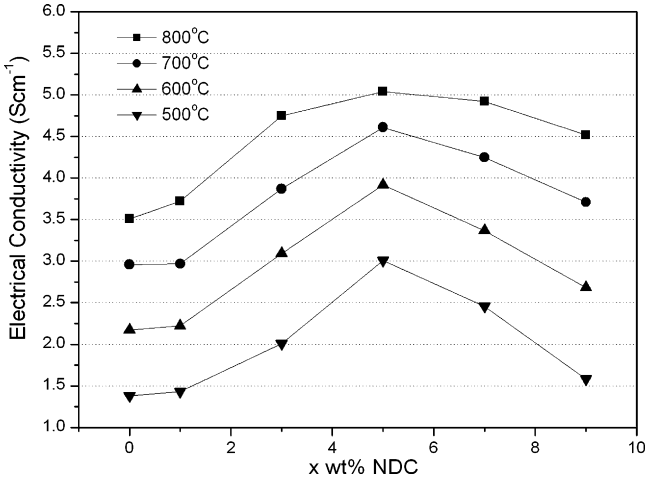

Fig. 7. Effect of NDC content on the electrical conductivity of the specimens in hydrogen at different temperatures.

the electrical conductivities of all the specimens with different NDC content, ranging from 3 wt% to 7 wt%, were more than 2.0 S cm^{-1} even at 500 °C in hydrogen, all these materials are suitable to be used as interconnect materials for IT-SOFCs. Therefore, significant reduction in operating temperature will dramatically reduce not only the cost of materials but also the cost of fabrication. Besides, under SOFC operating environments, interconnect must exhibit excellent electrical conductivity preferably with nearly 100% electronic conduction. In an ideal situation, the ohmic loss due to the introduction of interconnect is noticeably small so that the power density of a stack does not show profound drop as compared to that of an individual cell. Thus, reducing the ohmic resistances is the effective way of enhancing the performance of SOFCs.

In summary, the electrical conductivity of the material has two different mechanisms. At the oxidizing atmosphere such as oxygen or air at the cathode, the conductivity is on account of the Cr^{3+} to Cr^{4+} transition via an electronic compensation mechanism. While in the reducing circumstance, such as in fuel gas at the anode, the conductivity is obviously retarded owing to the appearance of oxygen vacancies via the ionic compensation mechanism.

3.4. Coefficient of thermal expansion

Since SOFCs operate at high temperatures and endure the repeated thermal cycles from room temperature to the operating temperature, interconnects must be thermally compatible with the other cell components. Therefore, the CTE of SOFC interconnects must be close to those of the other cell components to minimize the thermal stresses. In Fig. 8, the thermal expansion of LCC was used as a control. The linear CTE of LCC is 11.12×10^{-6} K^{-1} in the temperature range of 30–1000 °C. With the increase of NDC content, the CTEs of specimens increased and reached the maximum when the NDC content is 9 wt%, indicating a distinct effect of NDC on the specimen's CTE. However, it can be seen that the CTEs of most specimens with different NDC contents (x = 1–5) are relatively close and very much compatible with other cell components, such as YSZ electrolyte (~10.5 ppm K^{-1}), Sr substituted $LaFeO_3$ cathode (11.9 ppm K^{-1}) and Ni-YSZ anode (10.8 ppm K^{-1}) used in SOFC. Therefore, it would be possible to minimize the thermal stress developed during the repeated thermal cycles of SOFC stack.

3.5. Oxygen penetration measurements

The interconnect plates for SOFC act as a complete gas barrier between fuel and air, therefore, high density is required after sintering at high temperature for SOFC. However, even if completely dense alkaline-earth-substituted lanthanum chromites are obtained, the partial reduction and oxygen vacancies at the reducing atmosphere may result in the oxygen permeation. Considering the changing of oxygen vacancies after introducing the NDC into LCC, we examined the oxygen penetration flux of the specimens sintered at 1400 °C for 4 h by gas chromatography. The oxygen pressures on the two sides of pellets were 8.61×10^{-4} atm and 0.25 atm, respectively. The average thickness of pellet is 1.16 mm. The oxygen permeation flux values at 800 °C are listed in Table 1. It clearly shows that the oxygen permeation flux increased with the increase of NDC content, ranging from 6.51×10^{-10} mol s^{-1} cm^{-2} (LCC without NDC) to the maximal value of 3.34×10^{-9} mol s^{-1} cm^{-2} (LCC with 9 wt% NDC) at 800 °C. Therefore, the efficiency loss of SOFC by permeation is negligible for the general cell design using LCC + NDC as interconnect.

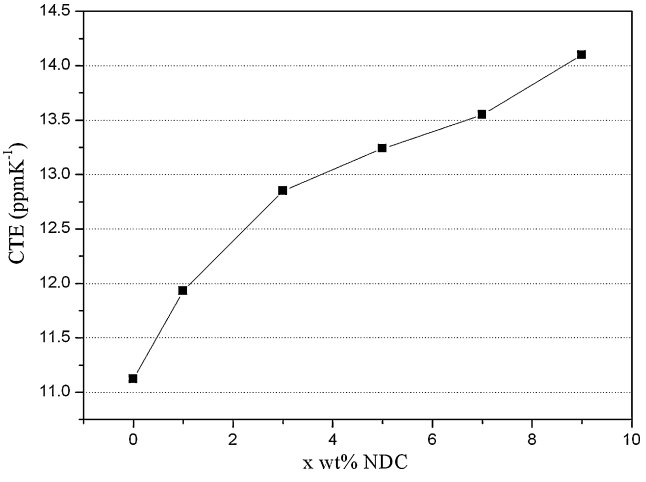

Fig. 8. The influence of NDC content on the CTE in the temperature range of 30–1000 °C in air.

4. Conclusions

The motivation for the study presented in this work was to improve the electrical property and sintering ability of the conventional interconnect $La_{0.7}Ca_{0.3}CrO_{3-\delta}$ and qualify there materials to be used at the intermediate temperatures. The addition of small amount $Ce_{0.8}Nd_{0.2}O_{1.9}$ with fluorite structure significantly improved the electrical conductivities and sintering ability of $La_{0.7}Ca_{0.3}CrO_{3-\delta}$. As for the specimen $La_{0.7}Ca_{0.3}CrO_{3-\delta}$ with 5 wt% $Ce_{0.8}Nd_{0.2}O_{1.9}$, the electrical conductivity at 800 °C in air reached 55.4 S cm^{-1}, which is 2.2 times as high as that of the commonly used lanthanum chromite $La_{0.7}Ca_{0.3}CrO_{3-\delta}$. At 500 °C, 600 °C and 700 °C, the electrical conductivities were 39.8 S cm^{-1}, 45.5 S cm^{-1} and 50.3 S cm^{-1}, respectively. At 800 °C in hydrogen, the specimen with 5 wt% $Ce_{0.8}Nd_{0.2}O_{1.9}$ has the maximum electrical conductivity of 5.0 S cm^{-1} which is also higher than that of $La_{0.7}Ca_{0.3}CrO_{3-\delta}$. At 500 °C, 600 °C and 700 °C, the maximal values of the electrical conductivities reached 3.0 S cm^{-1}, 3.9 S cm^{-1} and 4.6 S cm^{-1}, respectively. Most CTEs of specimens with different $Ce_{0.8}Nd_{0.2}O_{1.9}$ content (1–5 wt%) were compatible with other cell components. The addition of $Ce_{0.8}Nd_{0.2}O_{1.9}$ increased the oxygen permeation ability; however, the values were still negligible for the general cell design. In summary, this materials system exhibited excellent electrical performance, very small oxygen permeation ability, high relative density, and matched thermal expansion with other cell components. These characteristics, especially the improved electrical conductivities in air and hydrogen as well as the sintering ability will enable the composite materials suitable as a high-performance interconnect for IT-SOFC.

Acknowledgements

This project is financially supported by Development Program for Outstanding Young Teachers in Harbin Institute of Technology (No. HITQNJS.2008.056), China Postdoctoral Science Foundation (No. 20070420865), and Natural Science Foundation of China (No. 50778053).

References

[1] S.C. Singhal, K. Kendal (Eds.), High Temperature Solid Oxide Fuel Cells: Fundamental, Design and Applications, Elsevier, 2003, pp. 15–55.
[2] S. de Souza, S.J. Visco, L.C. De Jonghe, Solid State Ionics 98 (1997) 57–61.
[3] S. de Souza, S.J. Visco, L.C. De Jonghe, J. Electochem. Soc. 144 (1997) L35.
[4] H. Ishihara, H. Matsuda, Y. Takita, J. Am. Chem. Soc. 116 (1994) 3801.
[5] M. Feng, J.B. Goodenough, Eur. J. Solid State Inorg. Chem. T31 (1994) 663.
[6] P. Huang, A. Petric, J. Electrochem. Soc. 143 (5) (1996) 1644.
[7] K.Q. Huang, R. Tichy, J.B. Goodenough, J. Am. Ceram. Soc. 81 (1998) 2565.
[8] W.Z. Zhu, S.C. Deevi, Mater. Sci. Eng. A 348 (2003) 227–243.
[9] N.Q. Minh, T. Takahashi, Science and Technology of Ceramic Fuel Cells, Elsevier, Amsterdam, 1995.

[10] Z. Yang, K.S. Weil, D.M. Paxton, J.W. Stevenson, J. Electrochem. Soc. 150 (9) (2003) A1188.
[11] A.L. Chick, J. Liu, W.J. Stevenson, et al., J. Am. Ceram. Soc. 80 (1997) 2109–2120.
[12] K. Oikawa, T. Kamiyama, T. Hashimoto, et al., J. Solid State Chem. 154 (2000) 524–529.
[13] N. Sakai, T. Kawada, H. Yokokawa, M. Dokiya, Solid State Ionics 40–41 (1990) 394–397.
[14] A. Chakraborty, R.N. Basu, H.S. Maiti, Mater. Lett. 45 (2000) 162–166.
[15] V.H. Schmidt, Electrical Properties of Lanthanum Chromite Based Ceramics in Hydrogen and Oxidizing Atmospheres of High Temperature, Rept. No. DOE/ET/15415, US Department of Energy, Washington DC, 1981.
[16] B.C.H. Steele, in: J.A.G. Drake (Ed.), Electrochemistry and Clean Energy, Royal Society of Chemistry, 1994, p. 8.
[17] H. Zhong, X. Zhou, X. Liu, G. Meng, J. Rare Earths 23 (2005) 36–40.
[18] C. Milliken, A. Khandkar, in: S.C. Singhal (Ed.), Proceedings of the 1st International Symposium on Solid Oxide Fuel Cells, The Electrochemical Society Proceedings Series, Pennington, NJ, 1989, p. 361.
[19] A. Chakraborty, P.S. Devi, S. Roy, H.s. Maiti, Mater. Lett. 20 (1994) 63–69.
[20] H. Zhong, X. Zhou, X. Liu, G. Meng, Solid State Ionics 176 (2005) 1057–1061.
[21] D.B. Meadowcroft, in: T. Gray (Ed.), International Conference on Strontium Containing Compounds, Atlantic Research Institute, Halifax, Canada, 1973, p. 119.
[22] B.F. Flandermeyer, M.M. Nasrallah, D.M. Sparlin, H.U. Anderson, High Temp. Sci. 20 (1985) 259.
[23] I. Yasuda, T. Hikita, J. Electrochem. Soc. 140 (1993) 1699.
[24] J. Mizusaki, S. Yamauchi, K. Fueki, A. Ishikawa, Solid State Ionics 12 (1984) 119.
[25] H.E. Hofer, W.F. Kock, J. Electrochem. Soc. 140 (1993) 2889.
[26] D.P. Karim, A.T. Aldred, Phys. Rev. B 20 (1979) 2255.
[27] S. Tao, J.T.S. Irvine, J. Electrochem. Soc. 151 (2) (2004) A252–A259.
[28] N.Q. Minh, C.R. Horne, F.S. Liu, D.M. Moffatt, P.R. Staszak, T.L. Stillwagon, J.J. VanAckeren, Proceedings of the 25th Intersociety Energy Convention Engineering Conference, vol. 13, American Institute of Chemical Engineers, New York, 1990, p. 256.